J Appl Physiol 121: 615–622, 2016.
First published July 8, 2016; doi:10.1152/japplphysiol.00080.2016.

Evaluating the control: minipump implantation and breathing behavior in the neonatal rat

Ian J. Kidder,[1] Jordan A. Mudery,[1] Santiago Barreda,[2] David J. Taska,[1] and E. Fiona Bailey[1]

[1]*Department of Physiology, College of Medicine, The University of Arizona, Tucson, Arizona; and* [2]*Department of Linguistics, University of California Davis, Davis, California*

Submitted 27 January 2016; accepted in final form 5 July 2016

Kidder IJ, Mudery JA, Barreda S, Taska DJ, Bailey EF. Evaluating the control: minipump implantation and breathing behavior in the neonatal rat. *J Appl Physiol* 121: 615–622, 2016. First published July 8, 2016; doi:10.1152/japplphysiol.00080.2016.—We evaluated genioglossus (GG) gross motoneuron morphology, electromyographic (EMG) activities, and respiratory patterning in rat pups allowed to develop without interference (unexposed) and pups born to dams subjected to osmotic minipump implantation in utero (saline-exposed). In *experiment 1*, 48 Sprague-Dawley rat pups (Charles-River Laboratories), ages *postnatal day 7* (P7) through *postnatal day 10* (P10), were drawn from two experimental groups, saline-exposed ($n = 24$) and unexposed ($n = 24$), and studied on P7, P8, P9, or P10. Pups in both groups were sedated (Inactin hydrate, 70 mg/kg), and fine-wire electrodes were inserted into the GG muscle of the tongue and intercostal muscles to record EMG activities during breathing in air and at three levels of normoxic hypercapnia [inspired CO_2 fraction (FI_{CO_2}): 0.03, 0.06, and 0.09]. Using this approach, we assessed breathing frequency, heart rate, apnea type, respiratory event types, and respiratory stability. In *experiment 2*, 16 rat pups were drawn from the same experimental groups, saline-exposed ($n = 9$) and unexposed ($n = 7$), and used in motoneuron-labeling studies. In these pups a retrograde dye was injected into the GG muscle, and the brain stems were subsequently harvested and sliced. Labeled GG motoneurons were identified with microscopy, impaled, and filled with Lucifer yellow. Double-labeled motoneurons were reconstructed, and the number of primary projections and soma volumes were calculated. Whereas pups in each group exhibited the same number ($P = 0.226$) and duration ($P = 0.093$) of respiratory event types and comparable motoneuron morphologies, pups in the implant group exhibited more central apneas and respiratory instability relative to pups allowed to develop without interference.

upper airway; motoneuron; apnea; control

NEW & NOTEWORTHY

Accumulating evidence indicates that gestational and/or neonatal stress perturbs central nervous system (CNS) development and that fetal exposure to anesthetic agents or narcotics disrupts critical processes of axonal growth and synapse elimination. Here we focus on processes related to minipump implantation surgery and the potential impact of implant surgery on early postnatal respiratory control and function.

OSMOTIC MINIPUMPS ARE small-capacity pumps (volumes 0.1–2.0 ml) that permit sustained drug administration at controlled rates over several days to weeks (23). Minipumps have been widely used to study effects of chronic nicotine exposure on the developing fetus and, more specifically, on the development of respiratory control and the regulation of respiratory motoneuron function (6, 7, 16, 24–26, 32, 34, 38, 39, 46, 47, 57). Given accumulating evidence that gestational and/or neonatal stress perturbs CNS development (17, 21, 23, 31, 40, 62) and, second, that fetal exposure to anesthetic agents or to narcotics can disrupt critical processes including neurotransmitter synthesis, neurogenesis, and myelination (56, 59, 60, 68, 69) and alter axonal growth and synapse elimination (15, 49), our focus in this case was on processes related to minipump implantation surgery and the potential impact on postnatal respiratory control and function. Accordingly, we studied pups born to dams that had undergone implant surgery and pups allowed to develop without interference, testing the null hypothesis that saline minipump implantation has no effect on respiratory patterning (9), on electromyographic activities of an airway dilator muscle (i.e., genioglossus) and respiratory pump muscles (i.e., internal and external intercostals), or on upper airway motoneuron morphology.

MATERIALS AND METHODS

All experimental procedures were approved by the Institutional Animal Care and Use Committee at the University of Arizona and adhered to the Public Health Service Policy on Humane Care and Use of Laboratory Animals. Forty-eight Sprague-Dawley rat pups (Charles-River Laboratories), ages *postnatal day 7* (P7) through *postnatal day 10* (P10), were drawn from two experimental groups, saline-exposed ($n = 24$) and unexposed ($n = 24$), and studied on P7, P8, P9, or P10. Pups were obtained from 14 litters each for saline-exposed and unexposed groups, with no more than 3 pups drawn from any litter. In this case, we used saline exposure to assess the effects of anesthesia and surgical procedures (see details below). Unexposed rat pups were allowed to develop without interference and served as the control group. Pups in both groups had access to their dam, and in turn, dams had access to food and water ad libitum. All animals were housed under a 12:12-h light/dark cycle.

Saline Exposure

We followed previously published procedures for minipump implantation (13, 19, 34, 35, 38, 39, 46, 47). Pregnant dams were delivered to the Animal Care facility at the University of Arizona and given 24 h to acclimate. On the following day, dams were anesthetized via intramuscular injection of 0.75 ml/kg "rabbit mix" (5-ml ketamine, 8-ml 20 mg/ml xylazine, 2-ml acepromazine) into the hind limb, followed by a subcutaneous injection of analgesic (Buprenex, 0.5 mg/kg) and preparation of the surgical site. An absence of limb withdrawal to paw pressure was confirmed prior to all surgical procedures and reassessed every 15 min to confirm a sufficient plane of anesthesia. A small incision was made at the base of the neck and stretched with a hemostat to facilitate implantation. An osmotic minipump (Alzet 2ML4; Durect, Cupertino, CA) was then placed through the incision and sutured shut (nylon). Antibiotics (Combi-Pen-48; Bimedi) were provided via a subcutaneous injection upon completion of the surgery. Postoperative care included analgesic

Address for reprint requests and other correspondence: E. F. Bailey, Dept. of Physiology, College of Medicine, The University of Arizona, 1713 E. University Blvd., Tucson, AZ 85721-0093 (e-mail: ebailey@email.arizona.edu).

injections (Buprenex, 0.5 mg/kg) every 12 h for a period of 36 h and an additional antibiotic injection 24-h postsurgery. Minipumps were charged to deliver saline at 6 $mg \cdot kg^{-1} \cdot day^{-1}$ for 28 days. All surgeries were performed on *embryonic day 5* to coincide with embryonic implantation in the uterine wall late on *gestational day 5* (67). Because the Alzet 2ML4 pump is capable of delivering this dose for a period of 28 days, pups were exposed to saline throughout gestation through to *postnatal day 10*.

Respiratory Experiments

Pups were sedated via intraperitoneal injections of barbiturate (70 mg/kg each, Inactin hydrate; Sigma-Aldrich) (43), and bipolar hook-wire electrodes (0.05 mm; California Fine Wire) were inserted into the genioglossus (GG) muscle and into internal and external intercostal (IC) muscles with a 30-Fr needle (11). The electrode tips were bared of insulation to increase recording "pick-up" area. An additional hook-wire electrode, inserted into the scruff of the neck, served as electrical ground. Electromyographic (EMG) signals were sampled at 5 kHz and preamplified at a head stage [model 1902-10, gain 10 times; Cambridge Electronic Design (CED)] and subsequently amplified (model 1902, gain 1,000 times; CED) and band-pass filtered (200–2,000 Hz). Following insertion of the electrodes, pups were placed supine on a platform in a flow-through chamber (Fig. 1) and maintained at 37 ± 0.9°C with a heating pad (IT-18; Physitemp Instruments). At the conclusion of the experiment, pups were euthanized by an intraperitoneal overdose of pentobarbital (0.05 ml of 260 mg/ml solution). Placement of EMG electrodes in both muscles was verified at the termination of the experiment via dissection.

Respiratory-related motions of the chest wall were detected by a force transducer (FORT100; World Precision Instruments) placed in contact with the chest wall. Chest wall motion was sampled at 5 kHz amplified (1,000 times, TBM4 M; World Precision Instruments, Sarasota, FL) and displayed in Spike2.0 (Cambridge Electronic Design) (Fig. 1). Pups breathed for 2 min in room air (baseline) and at each of three levels of normoxic hypercapnia [0.03, 0.06, and 0.09 inspired CO_2 fraction ($F_{I_{CO_2}}$)]. Humidified gases were delivered into the flow-through chamber via a rotameter (model FM-1050-VO-3T; Matheson Tri-gas). The composition of the inspired gas was monitored online using O_2 and CO_2 gas analyzers (VacuMed 17518 and 17515). Temperature and humidity were monitored with a thermometer hygrometer (Fluker's CF-22642). All experimental sessions were captured using a Microsoft LifeCam Studio webcam connected to the experiment computer and synchronized with experimental data (Spike2.0, version 7.2). We used this footage to verify apneas and to distinguish nonrespiratory movement-related artifacts according to previously established criteria (20).

Labeling Experiments

To determine the effects of osmotic minipump implantation on motoneuron cell morphology, we performed motoneuron-labeling experiments on 16 pups from unexposed ($n = 7$) and saline-exposed ($n = 9$) litters. As for in vivo measures, two to three pups were selected at random from each litter with no more than three motoneuron fills examined per animal. Injections of 10 μl of rhodamine dextran (tetramethylrhodamine dextran; Invitrogen, Carlsbad, CA) dissolved in deionized water were delivered into the GG muscle via Hamilton syringe (26 gauge, 10 μl; Hamilton, Reno, NV). Two days following the injection, pups were euthanized via lethal injection of sodium pentobarbital. Pups were decerebrated at the coronal suture and eviscerated, and the brain, brain stem, tissue surrounding spinal column, and rib cage were transferred to a dish filled with chilled (4°C) artificial cerebral spinal fluid (aCSF) solution. The medulla and spinal cord were extracted and pinned to a cutting block for serial sectioning via vibratome (Vibratome 3000; The Vibratome Company, St. Louis, MO). Transverse sections were taken until the rostral inferior olive and obex were visible. Two 500-μm sections were collected, which included the obex and the hypoglossal motor nucleus (5, 39). Sections were fixed overnight in dark conditions at 4°C in 4% paraformaldehyde (PFA) 0.1 M PBS (Sigma-Aldrich) solution.

Fixed sections were placed on a Leitz Laborlux S compound microscope equipped with epifluorescent illumination and filter sets for Lucifer yellow and rhodamine dextran (Leitz, Weitz, Germany). Glass electrodes (model p-97 Flaming/Brown micropipette puller) were used to impale a rhodamine dextran-labeled cell under visual

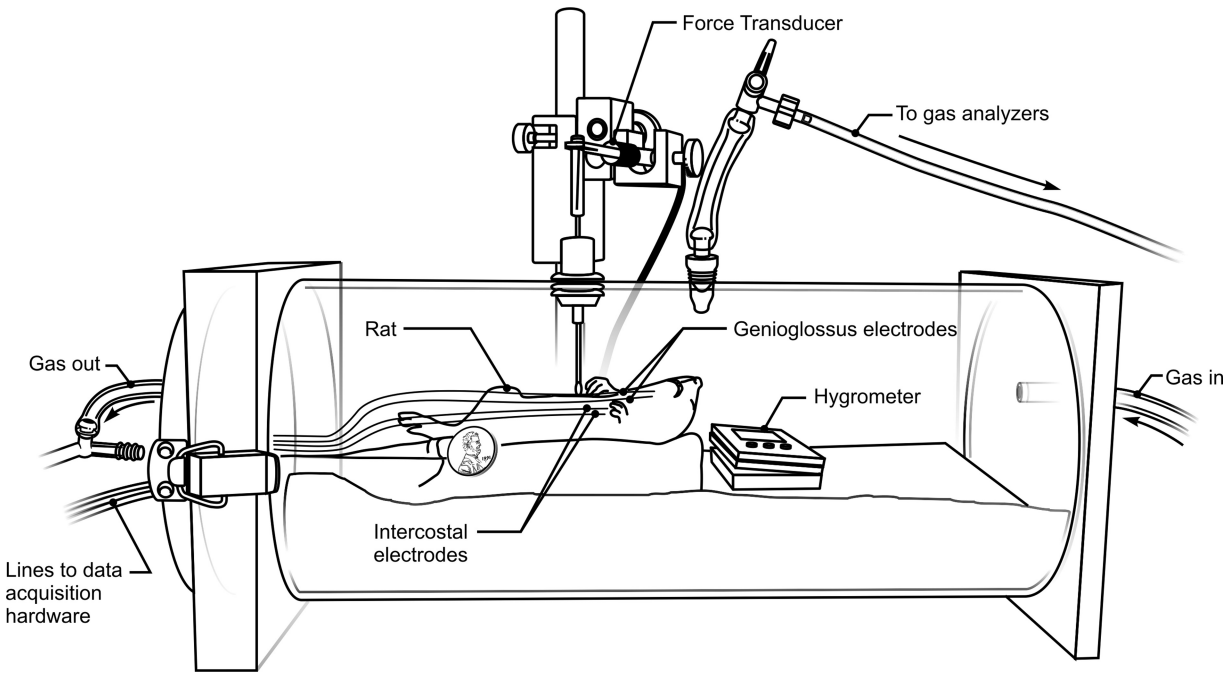

Fig. 1. Experimental schematic of whole body flow through chamber setup, showing location of the force transducer used to detect chest wall motions and genioglossus and intercostal electromyographic electrode locations.

control using a manual micromanipulator (Leitz). Each electrode was filled with 8% Lucifer yellow in lithium chloride (1.0 M). The interior of the micropipette was connected to the amplifier via an Ag/Ag Cl wire, and the bath was grounded similarly. Dye was introduced into the cell by passing negative current through the electrode for 20–30 min to facilitate intracellular filling. The brain stem section was then stored in dark conditions at 4°C in 4% PFA in 0.1 M PBS. Sections subsequently were removed from PFA and washed four times in fresh 0.1 M PBS for 15 min at 4°C. Sections then were cleared in 50% glycerol 0.1 M PBS for 2 h, followed by 2 h in 80% glycerol 0.1 M PBS. Sections were mounted and stored in dark conditions at 4°C until imaging.

Confocal Imaging

Initial images were taken with a ×20 nonimmersion lens to confirm cells were labeled with rhodamine dextran. Imaged z-stacks subsequently were collected using a Zeiss 510 laser scanning confocal microscope. A z-stack was obtained with a ×40 oil immersion lens and 458-nm laser excitation to visualize Lucifer yellow emissions. Subsequently, slices were visualized by excitation at 488 and 543 nm to observe emissions from Lucifer yellow and rhodamine dextran-filled cells.

Data Analysis

Respiratory-related measures. Respiratory-related data were recorded using Spike2 software (Cambridge Electronic Design) and analyzed off-line using custom programs within Spike2. A cessation in breathing (i.e., absence of chest expansion) lasting for two or more breath cycles was designated an apneic event (34). If EMG activity in both upper airway and respiratory pump muscles was quiescent during the event, it was designated as a central apnea (30, 43). If EMG activity persisted in pump muscles, accompanied by a decrease or absence of EMG activity in the upper airway muscle, the event was designated as a hypopnea (30, 43, 53, 54, 58). Mixed apneas were events characterized by an absence of EMG activity in both upper airway and respiratory pump muscles (i.e., central apnea), followed by respiratory pump muscle recruitment with absent or reduced upper airway activity (i.e., hypopnea). Event duration was calculated (in s) as the interval before resumption of normal, eupneic breathing. Event types were assessed over 8 min, corresponding to 2-min breathing in room air and 3, 6, and 9% $F_{I_{CO_2}}$. Breathing rates were determined as the number of chest wall expansions (inspirations) per minute epoch. Heart rates were determined from the ECG signal obtained from the intercostal EMG lead, and R wave events were discriminated from the lead signal and reported per minute epoch. Finally, estimates of respiratory stability were obtained from the deidentified and digitized chest wall traces. The autocorrelation function (ACF) was applied to each respiratory trace using a 10-s (5,001 sample) window that encompassed at least 18 breaths devoid of spontaneous apneas/hypopneas and movement-related artifact.

GG motoneuron morphology. Three-dimensional reconstructions of double-labeled cells were created from z-stacks using proprietary software (Reconstruct version 1.1.0.1; National Institutes of Health). All reconstructions were performed on fixed tissues after histochemical reactions, dehydration, and clearing. The area of the soma was traced for each plane within a z-stack and subsequently reconstructed (Imaris; Bitplane, Concord, MA). The number of primary projections—defined as a dendrite connected to the soma prior to the first branch point—was counted at the boundary of the cell body, and estimates of soma volume and soma surface area were determined by adding cross-sectional areas obtained in each plane and for each z-stack.

Statistics. With the exception of cell volume and surface areas, results are expressed as means ± SE; *n* refers to the number of cells or animals as indicated. For statistical calculations we used SigmaStat 3.11 (Systat Software, Chicago, IL). A univariate ANOVA was used to test for group differences in body mass. The effects of group (i.e., saline-exposed vs. unexposed), gas condition (i.e., room air, 0.03, 0.06, 0.09 $F_{I_{CO_2}}$), and age (P7, P8, P9, P10) on heart rate and breathing frequency were assessed via a general linear ANOVA and a mixed model ANOVA for respiratory event frequency. A chi-square statistic (likelihood ratio) was used to assess differences in apnea type between groups. Differences in respiratory patterning were assessed via repeated measures ANOVA with one between-subjects factor, experimental group, and one within-subject factor, breath distance. Greenhouse-Geisser corrections for heterogeneity of between-group variances (sphericity) were employed as appropriate (29). Values derived from soma volume measures were compared between unpaired groups using the Mann-Whitney test for nonparametric data. All tests were performed using statistical software (SPSS and R) with significance level set at $P < 0.05$.

RESULTS

Mean data for body mass are presented in Table 1. There was no effect of group on body mass ($P = 0.174$), and pups in both groups made steady gains in weight with age ($P < 0.001$). There were no between-group differences in breathing frequency at baseline ($P = 0.512$). Average breathing frequencies at baseline were 105.33 ± 8.77 breaths/min for saline-exposed and 104.17 ± 11.08 breath/min for unexposed pups on P7. Basal breathing frequency rose steadily reaching 129.67 ± 20.14 breaths/min (unexposed) and 124.33 ± 14.19 breaths/min (saline-exposed) on P10. Heart rate paralleled respiration with no significant between-group differences at baseline ($P = 0.064$). The average heart rate rose from 362.50 ± 20.32 (saline-exposed) and 350.08 ± 34.28 (unexposed) on P7 to 383.16 ± 24.34 (saline-exposed) and 373.46 ± 29.33 (unexposed) on P10. Although average heart rate and average breathing frequency both declined in hypercapnia ($P < 0.001$), there were no between-group differences in the magnitude of those declines (heart rate, $P = 0.414$; breathing frequency, $P = 0.100$; data not shown).

We identified a total of 43 respiratory events in pups from both groups although the count varied between pups of the same age. Because respiratory event frequency was unaffected by chemoreceptor stimulation, we collapsed results obtained across gas conditions and found no evidence of a between-group difference in the absolute number or duration of the events (Fig. 2). Using a previously reported technique (43), we subsequently differentiated between event types on the basis of chest wall motion and upper airway and respiratory pump muscle EMG. Illustrative recordings obtained from upper airway and pump muscle activities in a saline-exposed pup are shown in Fig. 3. In this example, a central apnea characterized by EMG inactivity in both the upper airway and respiratory

Table 1. *Body mass as a function of age and experimental group*

Age	Body Mass, g	
	Unexposed	Saline-Exposed
P7 ($n = 6$)	17.78 ± 1.02	17.60 ± 0.57
P8 ($n = 6$)	20.08 ± 1.07	21.20 ± 0.63
P9 ($n = 6$)	23.13 ± 1.84	24.97 ± 1.53
P10 ($n = 6$)	27.06 ± 2.39	24.78 ± 1.93

Values are means ± SE. There were no significant differences between groups ($P = 0.174$), and pups in both groups showed gains in mass with postnatal age ($P < 0.001$).

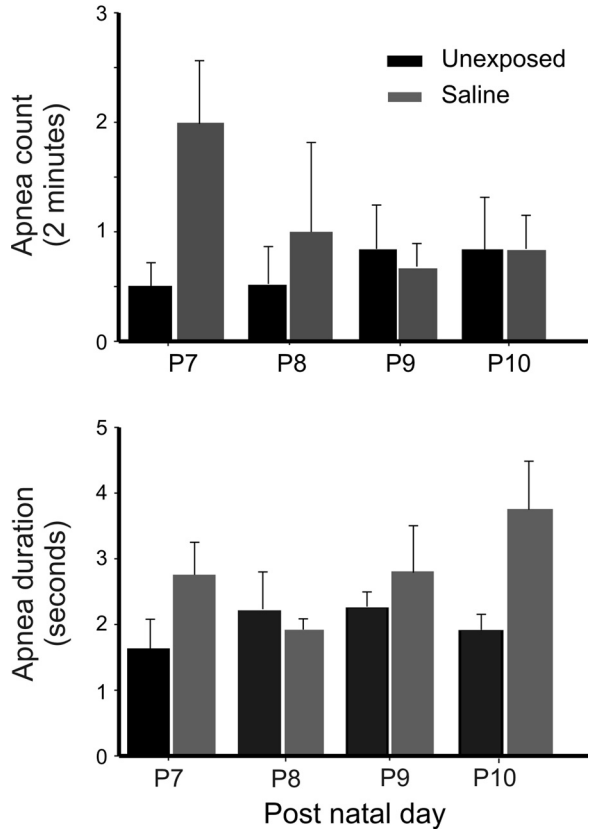

Fig. 2. Average number (± SE) of central apneas recorded in 2-min recording windows exhibited by saline-exposed ($n = 24$) (gray bars) and unexposed ($n = 24$) (black bars) pups spanning *postnatal days 7–10* (P7–P10). There were no significant differences detected between saline-exposed and unexposed pups in regard to either apneic frequency ($P = 0.226$) or apnea duration ($P = 0.725$) across the age span.

pump muscles is followed by sustained pump muscle activation in the absence of upper airway activity, consistent with a hypopnea. Here we define a respiratory event that progresses from central apnea to hypopnea as a mixed apnea.

Pups at all ages exhibited spontaneous apneas; however, the number of apneas varied between pups of the same postnatal age and as a function of experimental group (range, 0–4 apneas per gas condition). A total of 24/37 events were recorded in saline-exposed pups, and 13/37 were recorded in unexposed pups (Table 2). Hypopneas were fewer in number, and the majority (3/4) occurred in unexposed pups. Two mixed apneas were noted, and both were recorded in saline-exposed pups. Because the number of apneas and hypopneas did not change with increments in respiratory drive, we collapsed across gas condition; nevertheless, neither apnea frequency nor apnea duration differed as a function of group ($P = 0.226$) or postnatal age ($P = 0.725$).

Next, to evaluate respiratory stability, we applied an ACF to each digitized chest wall trace. Representative chest wall recordings and resultant autocorrelation functions are presented in Fig. 4 for unexposed (Fig. 4*A*) and saline-exposed (Fig. 4*B*) pups of the same age. In both examples, the respiratory traces are near periodic, and the trajectory of the chest wall excursion in each breath is similar, although not identical, to that of the preceding and subsequent breaths. The extent to which the original chest wall signal (solid trace) aligns with a lagged copy of the signal (dashed trace) varies as a function of the delay, with maximum alignment attained at a time point that corresponds to the signal period (P) and which corresponds to the pup's breathing frequency. A maximal signal alignment is reflected in local maxima in the ACF whereas poor signal alignment is reflected in time points between peaks in the ACF.

A comparison between the panels in Fig. 4 highlights subtle differences in respiratory patterning for unexposed and saline-exposed pups. Relative to the unexposed pup (Fig. 4*A*), there is greater misalignment evident between the chest wall trace and the lagged copy of the trace in the saline-exposed pup (Fig. 4*B*) that results in lower overall ACF peak values. Thus the first peak in the ACF (Fig. 4, *Ae* and *Be*) for the saline-exposed pup is low (~0.22) and roughly one-third that of the first peak in the ACF in the unexposed pup of the same age. Likewise, whereas the second peak in the ACF obtained from an unexposed pup is ~0.4, the second peak in a saline-exposed pup of the same age is less than half that value (~0.18). Poor signal alignment and lower average ACF peak values are features of saline-exposed pups and are indicative of greater respiratory instability relative to unexposed peers.

We used an ANOVA to evaluate between-group differences in respiratory stability and to evaluate the ACF for each rat as a function of breath distance. ACF values for individual (saline-exposed and unexposed) pups along with group average (± SE) ACFs for are shown in Fig. 5*A*. A significant main effect for group [$F(1,44) = 6.11$, $P = 0.017$] indicates that saline-exposed pups experience greater respiratory instability than unexposed peers. Figure 5*B* shows the time course of respiratory instability, i.e., how quickly it develops and how quickly it resolves. The results of the ANOVA confirm a significant main effect for breath distance [$F(4,176) = 140.89$, $P < 0.001$]; however, the absence of an interaction [$F(4,176) = 0.39$, $P < 0.82$] indicates that the time course of that instability is similar for saline-exposed and unexposed pups.

Last, we examined the gross motoneuron morphology of retrogradely labeled genioglossus motoneurons and obtained estimates of soma volume and primary dendrite number for a subset of pups in both groups (Table 3). Fills obtained from saline-exposed pups exhibited the same number of primary dendrites relative to unexposed pups of the same age (5.3 ± 1.4 vs. 5.5 ± 0.8). A Mann-Whitney *U*-test was run on filled cells obtained from nine pups assessing differences in soma volume

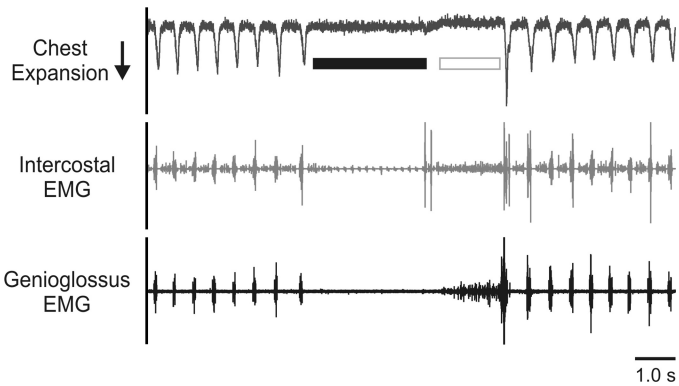

Fig. 3. An illustrative recording of a mixed apnea characterized by absence of EMG activity in pump and upper airway muscles followed by increasing EMG activation in both muscles followed by airway reopening and resumption of breathing. Black bar, central apnea; white bar, hypopnea.

Table 2. *Apneas were designated as central, hypopneas, or mixed on the basis of upper airway (genioglossus) and pump (intercostal) muscle EMG activity*

Group	Total	Respiratory Event Type		
		Central Apnea	Hypopnea	Mixed Apnea
Unexposed (n = 24)	16	13 (81%)	3 (19%)	0 (0%)
Saline-exposed (n = 24)	27	24 (89%)	1 (4%)	2 (7%)

Central apneas were most common, and the greatest proportion of mixed apneas occurred in saline-exposed pups.

and surface area (P = 0.05). Median scores in saline-exposed pups for soma volume and surface area were 10,053 μm^3 and 2,513.3 μm^2, respectively, compared with 15,500 μm^3 and 3,123.6 μm^2 in unexposed pups of the same age. Neither difference attained statistical significance (P = 0.27 and P = 0.54; data not shown).

DISCUSSION

Minipumps provide a means of delivering substrate on a controlled and continuous basis with minimal stress to the pregnant dam. For the majority, the control condition entails implantation of a minipump charged to deliver saline. To our knowledge, only one previously published study included a no-treatment or unexposed condition in which pregnant dams were free from any form of intervention (39). That study reported no evident differences in results obtained from saline-exposed and unexposed in vitro preparations.

In this case, our objective was to determine how processes related to implant surgery, i.e., anesthesia, analgesia, and/or maternal stress, impact upper airway muscle function and respiration-related parameters of developing pups in vivo. Importantly, values for respiratory event frequency and duration obtained under sedation are in good agreement with results obtained in awake and unsedated rats of the same age (34), and all pups exhibited a range of respiratory event types that encompassed central apneas, hypopneas, and mixed apnea. Equally important for the validity of the implant model, gross genioglossal motoneuron morphology and function—assessed via whole muscle EMG—appear comparable for saline-exposed and unexposed neonates. Only two significant differences were noted, as follows: the absolute number of central apneas detected and the tendency toward respiratory instabil-

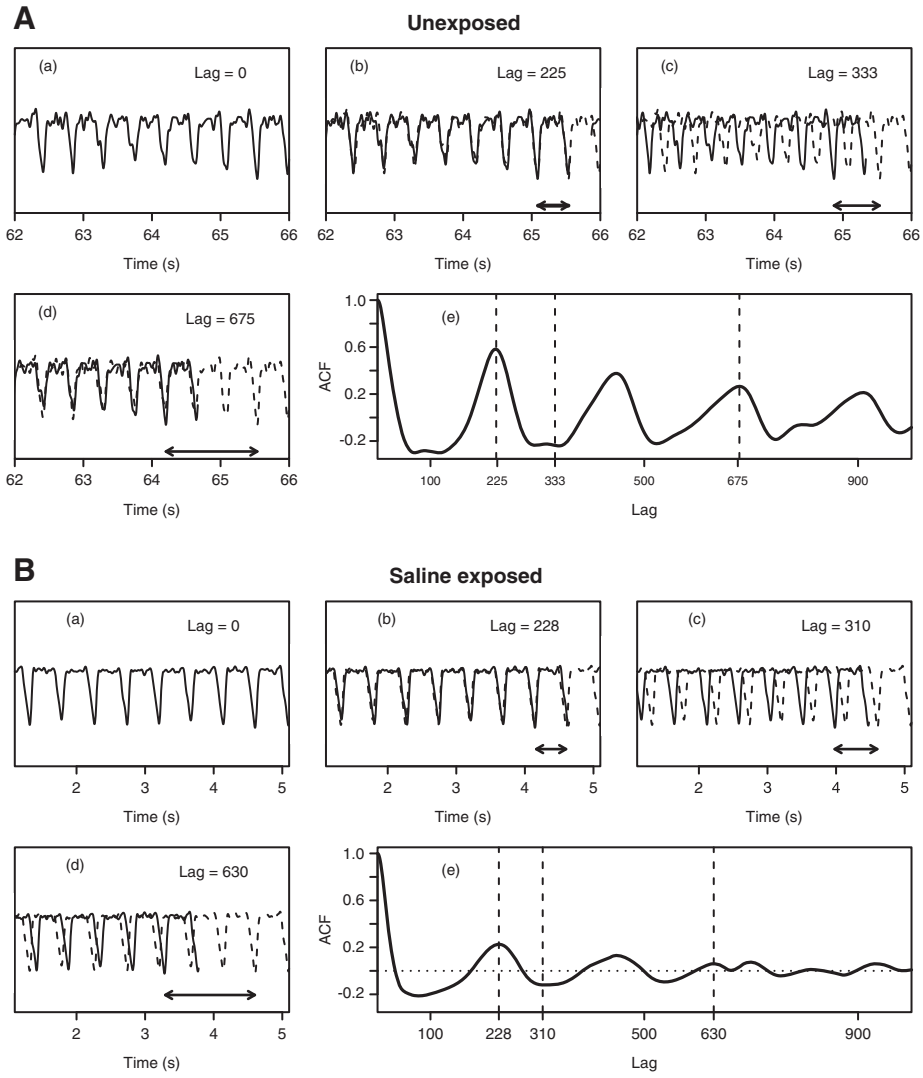

Fig. 4. Original chest wall recordings obtained from an unexposed (*A*) and a saline-exposed (*B*) pup. Solid lines show the respiratory trace, with a lagged or time-delayed copy of the trace indicated by a dashed trace. In each case, the offset between the traces is a result of the lag, the magnitude of which is represented by the horizontal arrows. Here, *b* and *d* in each panel show traces at lags equal to integer multiples of the period, and *c* shows the shift of an incomplete number of cycles in each case (unexposed and saline exposed) and highlights how well previous respiratory behavior predicts future respiratory behavior. Shown in *e* are the ACFs of the entire recording for unexposed and saline-exposed pups. Vertical dashed lines highlight peaks in each ACF the magnitude of which indicate how well actual and predicted chest wall traces align at each of the time points displayed in *b–d*.

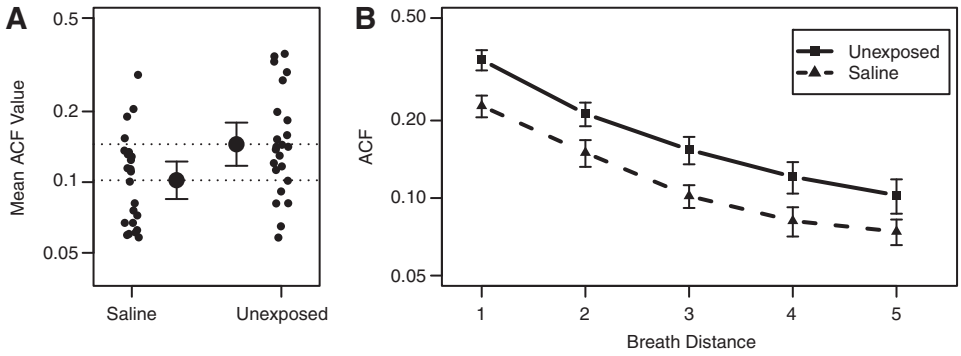

Fig. 5. *A*: individual ACF values for saline-exposed and unexposed pups displayed side by side with group average (± SE) ACF values. Relative to unexposed pups, saline-exposed pups exhibit overall lower average ACF values indicative of lower respiratory stability both within and across breaths (*$P = 0.017$). *B*: distribution of ACFs as a function of breath number and treatment group shows comparable rates of decline in stability as a function of the time ($P < 0.001$). Thus, once instability is triggered, the trajectory of that instability and the subsequent return to eupneic breathing is comparable for both groups.

ity, both of which were greater in the saline-exposed pups. The implications of these findings are discussed below.

Genioglossus Motoneurons

We report here on the motoneuron morphology and EMG activity recorded from the genioglossus muscle, previously identified as an airway dilator, and one of several tongue muscles that play a key role in preserving airway patency (3, 4, 41). We studied rat pups in the early postnatal period, well after GG motoneurons have completed their migration to the ventral subcompartment of the hypoglossal motor nucleus (48, 64–66). Importantly, the second week after birth coincides with maturation of the respiratory motor pattern (37) and encompasses a highly plastic and narrow window of adjustment in ventilation and metabolism (18, 45). Although numerous other studies document respiratory measures in pups as young as P3 (7, 35, 50), we were unsuccessful in extending the lower age boundary below P7. Because insertion of hook-wire electrodes is noxious, we found it necessary to sedate pups to minimize distress and movement-related artifact. Also, whereas the titration of sedation in pups at this developmental age and weight (<17 g) can be challenging, placement of electrodes into target muscle groups is extremely difficult in very young pups as the risk of pneumothorax and/or laryngeal spasm secondary to electrode insertion increases within the youngest age ranges.

We confirmed electrode placement within the GG at the termination of all experiments (2, 27, 43) and used that location to guide injections of rhodamine dextran label into the muscle. Motoneuron fills were performed on fixed tissue to limit the potential for swelling with the introduction of Lucifer yellow. Although the glycerol preparation can contribute to tissue shrinkage or expansion, because all slice sections were subject to the same treatment the effect is presumed comparable for all the tissue sections obtained (12, 52).

Table 3. *Reconstructions of double-labeled cells created from z-stacks using proprietary software showing comparable values for soma volume, surface area, and primary dendrite number for saline-exposed and unexposed pups ($P = 0.59$)*

	Motoneuron Morphology		
Group	Soma Volume, μm³	Soma Surface Area, μm²	Number of Dendrites
Unexposed ($n = 9$)	14,805.4 ± 5,283.2	3,074.54 ± 847	5.3 ± 1.4
Saline-exposed ($n = 7$)	10,330.9 ± 1,448.6	2,710.14 ± 363	5.5 ± 0.8

Values are means ± SD. Proprietary software, Reconstruct version 1.1.0.1, National Institutes of Health.

The techniques used in this study are comparable with earlier studies that assessed GG motoneuron morphology also in fixed tissue and which reported the same number of primary dendrites but smaller soma surface areas for neonates on P5–P6 and P13–P15 (51, 52). In contrast, our results both for volume and dendrite number correspond very well with the recently published work by Carrascal et al. for the same period, P6–P10 (18). However, it is unclear from that study whether rhodamine dextran was injected into the tongue body or into the extralingual GG; thus the possibility that intrinsic muscle motoneurons (verticalis, transversus, inferior and superior longitudinalis) were labeled cannot be ruled out. Given differences in the absolute size and body weights of neonatal rat and mouse at the same developmental age, it is unsurprising that average soma volumes and surface areas reported in our rodent pups are much larger than those reported recently by Kanjhan et al. in neonatal mice (42). The average ranges reported here for soma volume (10,330–14,850 μm^3) and surface area (2,710–3,074 μm^2) in the neonatal rodent are larger than the values recently reported by Kanjhan et al. for P5–P8 and P9–P13 mice (i.e., soma volume, 4,824–6,013 μm^3; soma surface area, 1,578-1,603 μm^2) (42) although the progression in size and volume with development appears consistent.

Implant Surgery

Consistent with previous studies, we administered an anesthetic comprising xylazine, ketamine, and acepromazine to each dam prior to surgery. A single dose of buprenorphine was administered for purposes of postoperative analgesia. Surgeries were performed on *gestational day 5* to coincide with embryonic implantation into the uterine wall (63). Some previous studies show adverse effects on fetal growth following repeat or sustained administration of buprenorphine and/or ketamine (33, 36). Buprenorphine is a long-acting agonist/antagonist of opioid receptors, and prenatal administration affects neurotrophic factor and neurotransmitter synthesis, neurogenesis, and myelination as well as axonal growth (56, 59, 60, 68, 69). Prenatal exposure to ketamine, which blocks *N*-methyl-D-aspartate (NMDA) glutamate receptors, also has been shown to interfere with synapse elimination, axonal growth (15, 49), and embryogenesis (1). Although neuronal susceptibility to insult varies with stage of development, in utero exposure to buprenorphine and/or ketamine may have contributed to the differences between saline-exposed and unexposed pups.

It seems unlikely that saline exposure might contribute to a change in respiratory behavior and/or respiratory stability. A recent study in neonatal mice failed to demonstrate any change in breathing frequency or minute ventilation following acute saline injection or saline infusion over 7 days (28). However, the potential for perioperative stress to impact fetal development is well documented, and acute stress has been shown to alter maternal endocrine function and, in turn, glucocorticoid signaling in the placenta as well as in the fetal brain (44). Although surgical implantation of the minipump was performed on *gestational day 5*, likely in advance of CNS development and synaptogenesis (55), maternal stressors including presurgical injection and/or physical restraint may impact fetal development resulting in altered postnatal function of saline-exposed pups (17, 62).

Central Apneas and Respiratory Instability

Subtle abnormalities in breath-to-breath interval variability have been documented in vivo (61) and in vitro (24); however, the frequency of abnormal respiratory events is remarkably low (6), and there is a pressing need for novel techniques to identify abnormal respiratory patterns. We developed a recording technique that permits the faithful tracking of chest wall motions even in very small pups (i.e., <30 g) (43). Here we applied a standard autocorrelation function to each digitized chest wall trace to obtain (unrestricted) estimates of respiratory system stability (9). The ACF is the Pearson product moment correlation of a signal with a time-delayed copy of itself and yields an estimate of where a data point will occur at (some) time later based on its current location. In this case, the series of individual data points represent the trajectory of the chest wall throughout the breath cycle, and the data series arising from each 2-min sample traced the trajectory of the chest wall through consecutive respiratory cycles. Unlike Poincaré plots that depict averages obtained from data points within a breath (10, 14, 22), the ACF considers each individual data point over successive breaths and therefore is exquisitely sensitive to any instability in chest wall motion. Using this approach, we detected instabilities in all pups with slightly more instability evident in the saline implant group than in unexposed peers. Unlike our previous results reported in pups exposed to nicotine in utero (9), here we found no difference between saline-exposed and unexposed pups in regard to the rate at which unstable breathing evolves. Thus, whereas respiratory instability is more common in saline-exposed pups, an instability, once triggered, follows the same time course for pups in both groups.

Summary

Laboratories worldwide use the neonatal rodent as a model to study the effects of acute and chronic drug exposure on cardiorespiratory development. The model is, in many respects, ideal because the fetus can be subjected to chronic drug/s exposure via an osmotic minipump implanted into the pregnant dam. Here we evaluated respiratory motoneuron morphology, respiratory event type (central apnea or hypopnea), event frequency, and respiratory stability in pups subject to minipump implantation during gestation and in pups allowed to develop without interference. Although we noted few between-group differences, evidence of a greater number of central apneas and greater risk for unstable breathing in saline implant pups reinforces the notion that gestational stress, anesthesia, and/or analgesia can impact fetal development and, in turn, breathing behavior in the first weeks of life.

DISCLOSURES

No conflicts of interest, financial or otherwise, are declared by the author(s).

AUTHOR CONTRIBUTIONS

I.J.K., J.A.M., S.B., and E.F.B. conception and design of research; I.J.K., J.A.M., and D.J.T. performed experiments; I.J.K., J.A.M., S.B., D.J.T., and E.F.B. analyzed data; I.J.K., J.A.M., S.B., and E.F.B. interpreted results of experiments; I.J.K., J.A.M., S.B., D.J.T., and E.F.B. prepared figures; I.J.K., J.A.M., S.B., and E.F.B. drafted manuscript; I.J.K., J.A.M., S.B., and E.F.B. edited and revised manuscript; I.J.K., J.A.M., S.B., D.J.T., and E.F.B. approved final version of manuscript.

REFERENCES

1. **Akeju O, Davis-Dusenbery BN, Cassel SH, Ichida JK, Eggan K.** Ketamine exposure in early development impairs specification of the primary germ cell layers. *Neurotoxicol Teratol* 43: 59–68, 2014.
2. **Bailey EF, Fregosi RF.** Coordination of intrinsic and extrinsic tongue muscles during spontaneous breathing in the rat. *J Appl Physiol (1985)* 96: 440–449, 2004.
3. **Bailey EF, Fregosi RF.** Pressure-volume behaviour of the rat upper airway: effects of tongue muscle activation. *J Physiol* 548: 563–568, 2003.
4. **Bailey EF, Huang YH, Fregosi RF.** Anatomic consequences of intrinsic tongue muscle activation. *J Appl Physiol (1985)* 101: 1377–1385, 2006.
5. **Ballanyi K, Ruangkittisakul A.** Structure-function analysis of rhythmogenic inspiratory pre-Botzinger complex networks in "calibrated" newborn rat brainstem slices. *Respir Physiol Neurobiol* 168: 158–178, 2009.
6. **Bamford OS, Carroll JL.** Dynamic ventilatory responses in rats: normal development and effects of prenatal nicotine exposure. *Respir Physiol* 117: 29–40, 1999.
7. **Bamford OS, Schuen JN, Carroll JL.** Effect of nicotine exposure on postnatal ventilatory responses to hypoxia and hypercapnia. *Respir Physiol* 106: 1–11, 1996.
9. **Barreda S, Kidder IJ, Mudery JA, Bailey EF.** Developmental nicotine exposure adversely effects respiratory patterning in the barbiturate anesthetized neonatal rat. *Respir Physiol Neurobiol* 208: 45–50, 2015.
10. **Barrett KT, Kinney HC, Li A, Daubenspeck JA, Leiter JC, Nattie EE.** Subtle alterations in breathing and heart rate control in the 5-HT1A receptor knockout mouse in early postnatal development. *J Appl Physiol (1985)* 113: 1585–1593, 2012.
11. **Basmajian JV.** Electromyography in normal intact mammals before and after birth. *Rev Can Biol* 21: 259–265, 1962.
12. **Berger AJ, Bayliss DA, Bellingham MC, Umemiya M, Viana F.** Postnatal development of hypoglossal motoneuron intrinsic properties. *Adv Exp Med Biol* 381: 63–71, 1995.
13. **Birnbaum SC, Kien N, Martucci RW, Gelzleichter TR, Witschi H, Hendrickx AG, Last JA.** Nicotine- or epinephrine-induced uteroplacental vasoconstriction and fetal growth in the rat. *Toxicology* 94: 69–80, 1994.
14. **Brennan M, Palaniswami M, Kamen P.** Poincaré plot interpretation using a physiological model of HRV based on a network of oscillators. *Am J Physiol Heart Circ Physiol* 283: H1873–H1886, 2002.
15. **Brewer GJ, Cotman CW.** NMDA receptor regulation of neuronal morphology in cultured hippocampal neurons. *Neurosci Lett* 99: 268–273, 1989.
16. **Campos M, Bravo E, Eugenin J.** Respiratory dysfunctions induced by prenatal nicotine exposure. *Clin Exp Pharmacol Physiol* 36: 1205–1217, 2009.
17. **Canan S, Aktas A, Ulkay MB, Colakoglu S, Ragbetli MC, Ayyildiz M, Geuna S, Kaplan S.** Prenatal exposure to a non-steroidal anti-inflammatory drug or saline solution impairs sciatic nerve morphology: a stereological and histological study. *Int J Dev Neurosci* 26: 733–738, 2008.
18. **Carrascal L, Nieto-Gonzalez JL, Cameron WE, Torres B, Nunez-Abades PA.** Changes during the postnatal development in physiological and anatomical characteristics of rat motoneurons studied in vitro. *Brain Res* 49: 377–387, 2005.
19. **Damaj MI, Kao W, Martin BR.** Characterization of spontaneous and precipitated nicotine withdrawal in the mouse. *J Pharmacol Exp Ther* 307: 526–534, 2003.

20. **Darnall RA, McWilliams S, Schneider RW, Tobia CM.** Reversible blunting of arousal from sleep in response to intermittent hypoxia in the developing rat. *J Appl Physiol (1985)* 109: 1686–1696, 2010.
21. **Delhaes F, Fournier S, Tolsa JF, Peyter AC, Bairam A, Kinkead R.** Consequences of gestational stress on GABAergic modulation of respiratory activity in developing newborn pups. *Respir Physiol Neurobiol* 200: 72–79, 2014.
22. **Dick TE, Mims JR, Hsieh YH, Morris KF, Wehrwein EA.** Increased cardio-respiratory coupling evoked by slow deep breathing can persist in normal humans. *Respir Physiol Neurobiol* 204: 99–111, 2014.
23. **Doucette TA, Ryan CL, Tasker RA.** Use of osmotic minipumps for sustained drug delivery in rat pups: effects on physical and neurobehavioural development. *Physiol Behav* 71: 207–212, 2000.
24. **Eugenin J, Otarola M, Bravo E, Coddou C, Cerpa V, Reyes-Parada M, Llona I, von Bernhardi R.** Prenatal to early postnatal nicotine exposure impairs central chemoreception and modifies breathing pattern in mouse neonates: a probable link to sudden infant death syndrome. *J Neurosci* 28: 13907–13917, 2008.
25. **Fregosi RF, Pilarski JQ.** Prenatal nicotine exposure and development of nicotinic and fast amino acid-mediated neurotransmission in the control of breathing. *Respir Physiol Neurobiol* 164: 80–86, 2008.
26. **Fuller DD, Dougherty BJ, Sandhu MS, Doperalski NJ, Reynolds CR, Hayward LF.** Prenatal nicotine exposure alters respiratory long-term facilitation in neonatal rats. *Respir Physiol Neurobiol* 169: 333–337, 2009.
27. **Gilliam EE, Goldberg SJ.** Contractile properties of the tongue muscles: effects of hypoglossal nerve and extracellular motoneuron stimulation in rat. *J Neurophysiol* 74: 547–555, 1995.
28. **Glausen T, Cunningham C, DeRuisseau L.** Confronting the effects of 0.9% saline administration on breathing. *FASEB J* 29: 2015.
29. **Greenhouse SW, Geisser S.** On methods in the analysis of profile data. *Psychometrics* 24: 95–112, 1959.
30. **Guilleminault C, Hill MW, Simmons FB, Dement WC.** Obstructive sleep apnea: electromyographic and fiberoptic studies. *Exp Neurol* 62: 48–67, 1978.
31. **Gulemetova R, Kinkead R.** Neonatal stress increases respiratory instability in rat pups. *Respir Physiol Neurobiol* 176: 103–109, 2011.
32. **Hafstrom O, Milerad J, Sandberg KL, Sundell HW.** Cardiorespiratory effects of nicotine exposure during development. *Respir Physiol Neurobiol* 149: 325–341, 2005.
33. **Hayashi H, Dikkes P, Soriano SG.** Repeated administration of ketamine may lead to neuronal degeneration in the developing rat brain. *Paediatr Anaesth* 12: 770–774, 2002.
34. **Huang YH, Brown AR, Costy-Bennett S, Luo Z, Fregosi RF.** Influence of prenatal nicotine exposure on postnatal development of breathing pattern. *Respir Physiol Neurobiol* 143: 1–8, 2004.
35. **Huang YH, Brown AR, Cross SJ, Cruz J, Rice A, Jaiswal S, Fregosi RF.** Influence of prenatal nicotine exposure on development of the ventilatory response to hypoxia and hypercapnia in neonatal rats. *J Appl Physiol (1985)* 109: 149–158, 2010.
36. **Hung CJ, Wu CC, Chen WY, Chang CY, Kuan YH, Pan HC, Liao SL, Chen CJ.** Depression-like effect of prenatal buprenorphine exposure in rats. *PLoS One* 8: e82262, 2013.
37. **Iizuka M.** Abdominal respiratory motor pattern in the rat. *Adv Exp Med Biol* 669: 157–161, 2010.
38. **Jaiswal SJ, Buls Wollman L, Harrison CM, Pilarski JQ, Fregosi RF.** Developmental nicotine exposure enhances inhibitory synaptic transmission in motor neurons and interneurons critical for normal breathing. *Dev Neurobiol* 76: 337–354, 2016.
39. **Jaiswal SJ, Pilarski JQ, Harrison CM, Fregosi RF.** Developmental nicotine exposure alters AMPA neurotransmission in the hypoglossal motor nucleus and pre-Botzinger complex of neonatal rats. *J Neurosci* 33: 2616–2625, 2013.
40. **Janus K.** Early separation of young rats from the mother and the development of play fighting. *Physiol Behav* 39: 471–476, 1987.
41. **John J, Bailey EF, Fregosi RF.** Respiratory-related discharge of genioglossus muscle motor units. *Am J Respir Crit Care Med* 172: 1331–1337, 2005.
42. **Kanjhan R, Fogarty MJ, Noakes PG, Bellingham MC.** Developmental changes in the morphology of mouse hypoglossal motor neurons. *Brain Struct Funct* (October 17, 2015). doi:10.1007/s00429-015-1130-8.
43. **Kidder IJ, Mudery JA, Bailey EF.** Neural drive to respiratory muscles in the spontaneously breathing rat pup. *Respir Physiol Neurobiol* 202: 64–70, 2014.
44. **Lan N, Chiu MP, Ellis L, Weinberg J.** Prenatal alcohol exposure and prenatal stress differentially alter glucocorticoid signaling in the placenta and fetal brain. *Neuroscience* (September 2, 2015). doi:10.1016/j.neuroscience.2015.08.058.
45. **Liu Q, Wong-Riley MT.** Gender considerations in ventilatory and metabolic development in rats: special emphasis on the critical period. *Respir Physiol Neurobiol* 188: 200–207, 2013.
46. **Luo Z, Costy-Bennett S, Fregosi RF.** Prenatal nicotine exposure increases the strength of GABA(A) receptor-mediated inhibition of respiratory rhythm in neonatal rats. *J Physiol* 561: 387–393, 2004.
47. **Luo Z, McMullen NT, Costy-Bennett S, Fregosi RF.** Prenatal nicotine exposure alters glycinergic and GABAergic control of respiratory frequency in the neonatal rat brainstem-spinal cord preparation. *Respir Physiol Neurobiol* 157: 226–234, 2007.
48. **Mazza E, Nunez-Abades PA, Spielmann JM, Cameron WE.** Anatomical and electrotonic coupling in developing genioglossal motoneurons of the rat. *Brain Res* 598: 127–137, 1992.
49. **Mickley GA, Lovelace JD, Farrell ST, Chang KS.** The intensity of a fetal taste aversion is modulated by the anesthesia used during conditioning. *Brain Res Dev Brain Res* 85: 119–127, 1995.
50. **Mortola JP, Lanthier C.** The ventilatory and metabolic response to hypercapnia in newborn mammalian species. *Respir Physiol* 103: 263–270, 1996.
51. **Nunez-Abades PA, Cameron WE.** Morphology of developing rat genioglossal motoneurons studied in vitro: relative changes in diameter and surface area of somata and dendrites. *J Comp Neurol* 353: 129–142, 1995.
52. **Nunez-Abades PA, He F, Barrionuevo G, Cameron WE.** Morphology of developing rat genioglossal motoneurons studied in vitro: changes in length, branching pattern, and spatial distribution of dendrites. *J Comp Neurol* 339: 401–420, 1994.
53. **Okabe S, Hida W, Kikuchi Y, Taguchi O, Takishima T, Shirato K.** Upper airway muscle activity during REM and non-REM sleep of patients with obstructive apnea. *Chest* 106: 767–773, 1994.
54. **Onal E, Leech JA, Lopata M.** Dynamics of respiratory drive and pressure during NREM sleep in patients with occlusive apneas. *J Appl Physiol (1985)* 58: 1971–1974, 1985.
55. **Palanisamy A.** Maternal anesthesia and fetal neurodevelopment. *Int J Obstet Anesth* 21: 152–162, 2012.
56. **Pettit AS, Desroches R, Bennett SA.** The opiate analgesic buprenorphine decreases proliferation of adult hippocampal neuroblasts and increases survival of their progeny. *Neuroscience* 200: 211–222, 2012.
57. **Pilarski JQ, Wakefield HE, Fuglevand AJ, Levine RB, Fregosi RF.** Increased nicotinic receptor desensitization in hypoglossal motor neurons following chronic developmental nicotine exposure. *J Neurophysiol* 107: 257–264, 2012.
58. **Remmers JE, deGroot WJ, Sauerland EK, Anch AM.** Pathogenesis of upper airway occlusion during sleep. *J Appl Physiol Respir Environ Exerc Physiol* 44: 931–938, 1978.
59. **Robinson SE.** Effects of perinatal buprenorphine and methadone exposures on striatal cholinergic ontogeny. *Neurotoxicol Teratol* 24: 137–142, 2002.
60. **Sanchez ES, Bigbee JW, Fobbs W, Robinson SE, Sato-Bigbee C.** Opioid addiction and pregnancy: perinatal exposure to buprenorphine affects myelination in the developing brain. *Glia* 56: 1017–1027, 2008.
61. **Schechtman VL, Lee MY, Wilson AJ, Harper RM.** Dynamics of respiratory patterning in normal infants and infants who subsequently died of the sudden infant death syndrome. *Pediatr Res* 40: 571–577, 1996.
62. **Schmitz C, Bultmann E, Gube M, Korr H.** Neuron loss in the mouse hippocampus following prenatal injection of tritiated thymidine or saline. *Int J Dev Neurosci* 17: 185–190, 1999.
63. **Serra A, Brozoski D, Hedin N, Franciosi R, Forster HV.** Mortality after carotid body denervation in rats. *J Appl Physiol (1985)* 91: 1298–1306, 2001.
64. **Smith JC, McClung JR, Goldberg SJ.** Effects of 12 days of artificial rearing on morphology of hypoglossal motoneurons innervating tongue retrusors in rat. *Anat Rec A Discov Mol Cell Evol Biol* 288: 280–285, 2006.
65. **Smith JC, McClung JR, Goldberg SJ.** Postnatal development of hypoglossal motoneurons that innervate the hyoglossus and styloglossus muscles in rat. *Anat Rec A Discov Mol Cell Evol Biol* 285: 628–633, 2005.
66. **Sokoloff AJ.** Topographic segregation of genioglossus motoneurons in the neonatal rat. *Neurosci Lett* 155: 102–106, 1993.
67. **Weitlauf HM.** Metabolic changes in the blastocysts of mice and rats during delayed implantation. *J Reprod Fertil* 39: 213–224, 1974.
68. **Wu CC, Hung CJ, Shen CH, Chen WY, Chang CY, Pan HC, Liao SL, Chen CJ.** Prenatal buprenorphine exposure decreases neurogenesis in rats. *Toxicol Lett* 225: 92–101, 2014.
69. **Wu VW, Mo Q, Yabe T, Schwartz JP, Robinson SE.** Perinatal opioids reduce striatal nerve growth factor content in rat striatum. *Eur J Pharmacol* 414: 211–214, 2001.